PRAMANA
—journal of
physics

© Printed in India

Vol. 48, No. 2,
February 1997
pp. 411–424

Resonances and chaos in the collinear collision system (He, H_2^+) and its isotopic variants

SUSANTA MAHAPATRA[a], N SATHYAMURTHY[a] and
RAMAKRISHNA RAMASWAMY[b]
[a] Department of Chemistry, Indian Institute of Technology, Kanpur 208 016, India
[b] School of Physical Sciences, Jawaharlal Nehru University, New Delhi 110 067, India

Abstract. The collinear atom-diatom collision system provides one of the simplest instances of chaotic or irregular scattering. Classically, irregular scattering is manifest in the sensitive dependence of post-collision variables on initial conditions, and quantally, in the appearance of a dense spectrum of dynamical resonances. We examine the influence of kinematic factors on such dynamical resonances in collinear (He, H_2^+) collisions by computing the transition state spectra for collinear (He, HD^+) and (He, DH^+) collisions using the time-dependent quantum mechanical approach. The nearest neighbor spacing distribution $P(s)$ and the spectral rigidity $\Delta_3(L)$ for these resonances suggest that the dynamics is predominantly *irregular* for collinear (He, HD^+) and predominantly *regular* for collinear (He, DH^+). These findings are reinforced by a significantly larger "correlation hole" in ensemble averaged survival probability $\langle\langle P(t)\rangle\rangle$ values for collinear (He, HD^+) than for collinear (He, DH^+). In addition we have also examined measures of classical chaos through the dependence of the final vibrational action, n_f, on the initial vibrational phase ϕ_i of the diatom, and Poincaré surfaces–of–section. They show that (He, HD^+) collisions are partly chaotic over the entire energy range (0–2.78 eV) while (He, DH^+) collisions, in contrast, are highly regular at collision energies below the classical threshold for reaction. Above the threshold, the scattering remains regular for initial vibrational states $v = 0$ and 1 of DH^+.

Keywords. Dynamical resonances; irregular scattering; collinear collisions.

PACS Nos 05.45; 34.10; 34.50

1. Introduction

Dynamical resonances in atom-molecule collisions [1] have been of great interest since they give rise to unusual variations in the scattering amplitude and related quantities. Reactive scattering resonances, which have been identified in a number of systems, one of which is (He, H_2^+) in collinear as well as noncollinear configurations [2], are characterized by oscillations in the reaction probability P^R as a function of the collision energy E. Many of them are of the Feshbach type and can be interpreted in terms of bound states supported by vibrational adiabatic potentials in hyperspherical coordinates [2(d),3]. A closer examination of $P^R(E)$ curves for collinear (He, H_2^+), for example, reveals that there are additional oscillations [2(h)] that are irregularly spaced as a function of the energy and which can not be assigned easily. The connection between such (quantal) resonances and the features of the classical dynamics is the subject of this article.

An investigation of quasi-classical trajectories [4] for the collinear

$$He + H_2^+ \rightarrow HeH^+ + H \qquad (R1)$$

reaction on the McLaughlin-Thompson-Joseph-Sathyamurthy (MTJS) potential energy surface (PES) [5] revealed that plots of final vibrational action (n_f) of the reactant/product molecule as a function of the initial vibrational phase (ϕ_i) of the reactant molecule consists of reactive (R) and nonreactive (NR) bands and a number of "chattering" or irregular trajectories in between. Upon magnification, it was found that the primary chattering region actually consists of a number of alternating R and NR bands with secondary chattering regions separating them. On further magnification, it became evident that there is a self-similar pattern repeating itself endlessly on increased resolution: $n_f(\phi_i)$ is a fractal [6] curve. Similar behavior has been found for several other systems like collinear (H, H_2) [7] and (Li, FH) [8]. Trajectories in the chattering regions tend to be chaotic, and the origin of classical chaos in collinear (He, H_2^+) system has been examined [9,10] by plotting the Poincaré surface of section (SOS) for a number of trajectories at energies below the reaction threshold.

It has been shown from time-dependent quantal wave packet (WP) calculations [2(h)] that the dynamics in collinear (He, H_2^+) collisions is "turbulent" when viewed in terms of probability density plots in configuration space. The transition state spectrum [11] is obtained by time evolving a wave packet centered in the interaction region, followed by computation of the Fourier transform of the autocorrelation function. Peaks in this spectrum correspond to dynamical resonances, and statistical analysis of the resonance energies, through the nearest neighbor spacing distribution (NNSD) or the spectral rigidity revealed an intermediate (partly regular and partly irregular) behavior for the system [12]. An ensemble averaged survival probability $\langle\langle P(t)\rangle\rangle$, computed [12] by Fourier transforming the spectral autocorrelation function to time domain followed by averaging over the initial states and Hamiltonian revealed the existence of a "correlation hole" that is graphic evidence for "irregularity" or quantum chaos [13–16]. A one-to-one correspondence between resonant periodic orbits (RPOs) and many transition state resonance eigenfunctions for the system also has been established [11, 17]. Therefore, on the whole, it could be concluded that there is a strong correlation between classical chaos, quantum chaos and dynamical resonances for systems like collinear (He, H_2^+).

Since dynamical resonances are intimately connected with the nature of the motion, it may be anticipated that kinematic factors play a crucial role in such systems. In the present study we report on the spectral characteristics and the behavior of quasiclassical trajectories for the two widely differing dynamical systems which arise from isotopic substitution of HeH_2^+, in order to investigate the role of kinematic factors in dynamical resonances. Within the Born-Oppenheimer approximation, isotopic substitution has no influence on the PES. Therefore, any difference in dynamical results must arise from the difference in masses of the atoms concerned.

We have computed the $P_v^R(E)$ curves for collinear He + HD^+ and He + DH^+ collisions, with HD^+ in different initial vibrational states, v, and find that $P_v^R(E)$ in either case behaves very differently [18] (from each other as well as from the case of HeH_2^+). Our results suggest that the wild oscillations in $P_v^R(E)$ may not necessarily mean that the

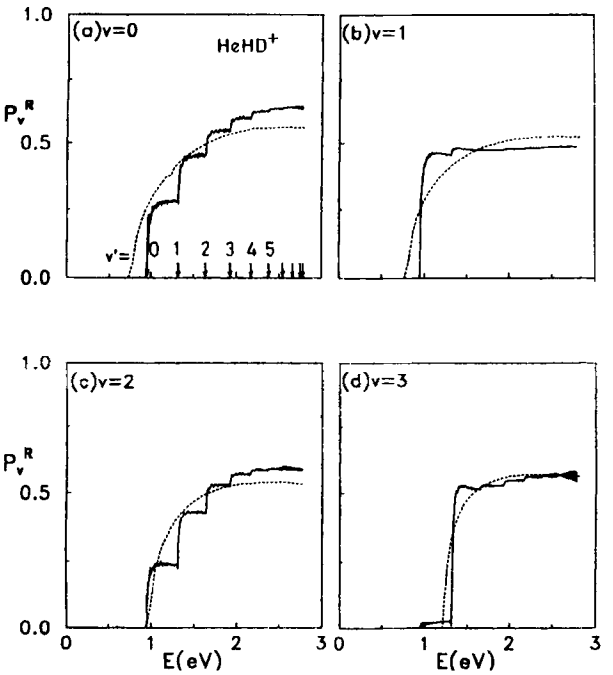

Figure 1. State-selected reaction probabilities (solid curve) computed from time-dependent quantal wave packet calculations and reproduced from Ref. [18] for different initial vibrational (v) states of HD^+ for the reaction $He + HD^+(v) \rightarrow HeH^+ + D$. The corresponding quasiclassical trajectory results are included as dashed curves. The threshold energies of various vibrational channels of the product HeH^+ are marked along the abscissa of panel (**a**) to illustrate the occurrence of sharp variations in P_v^R near each channel threshold.

dynamics is chaotic from a quantal point of view. Collinear (He, HD^+) would correspond to a **(H, LH)** mass combination, while (He, DH^+) would, to a **(H, HL)** mass combination. Here **H** and **L** refer to heavy and light atoms, respectively. Based on the known $P_v^R(E)$ results for other systems of **(H, LH)** type, it is expected that (He, HD^+) would have an oscillatory $P_v^R(E)$ as a light atom is exchanged between two heavy atoms, and that (He, DH^+) would have a relatively structureless $P_v^R(E)$ since the leaving atom is light. However, we find that $P_v^R(E)$ for collinear (He, HD^+) has a staircase-like structure, with minor oscillations about each "step", as illustrated in figure 1 for different initial v states of HD^+. The sharp variations in $P_v^R(E)$ (from one step to another) can be readily identified [18] as threshold resonances [19] corresponding to the opening up of either reactant or product vibrational channels. The undulations of smaller magnitude about the steps are due to the weak dynamical resonances found in the transition state spectrum. The $P_v^R(E)$ curve for collinear (He, DH^+) collisions, on the other hand, is highly oscillatory as shown in figure 2 and such an interpretation would not suffice to explain the structure. We therefore examine the transition state spectra of both systems for signatures of quantum chaos, and find that collinear (He, HD^+) collisions are predominantly chaotic, whereas (He, DH^+) collisions

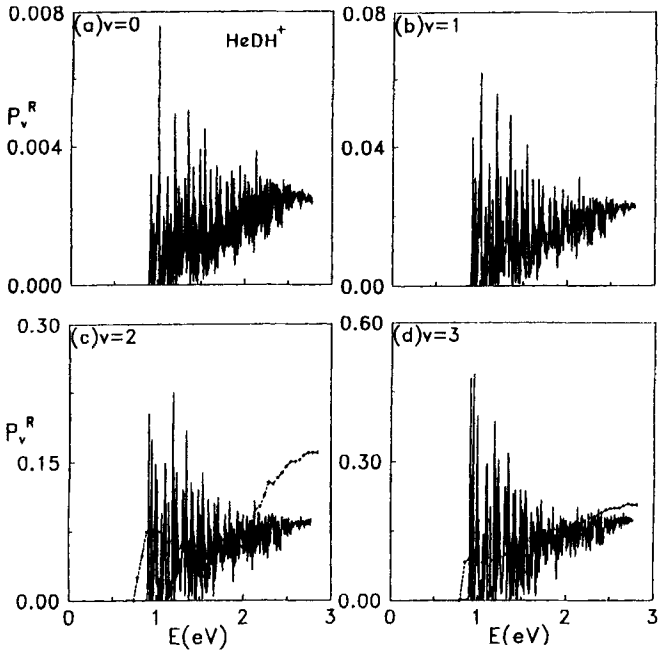

Figure 2. State-selected quantal reaction probabilities (solid curve) reproduced from Ref. [18] for the reaction $He + DH^+(v) \rightarrow HeD^+ + H$. The corresponding quasiclassical trajectory results are included as dashed curves. For $v = 0$ and 1, the quasiclassical trajectory calculations yield $P_v^R = 0$ (the statistical uncertainty level is 0.001).

are not. From a classical point of view, however, both systems show characteristics of chaos, albeit to different degrees.

2. Quantum chaos

We obtain the transition state spectra [18] for collinear (He, HD^+) and (He, DH^+) collisions by evolving a wave packet $\psi(t = 0)$ initially centered in the transition state region and computing the autocorrelation function $C(t) = \langle\psi(0)|\psi(t)\rangle$, and its Fourier transform. There are a large number of quasibound states, i.e. transition state resonances for both systems. These resonance energies $\{E_i, i = 1, 2 \ldots N\}$ provide the data for our subsequent analysis. Over the past couple of decades, considerable evidence has accumulated to support the hypothesis that the statistical properties of the eigenvalues of systems that have chaotic classical limits are identical to those of ensembles of random matrices [20] of the appropriate symmetry or universality class. Here we apply such analysis to the systems at hand.

The cumulative level density $N(E)$, which is a staircase function, is first unfolded in order to make the average density of energy levels uniform over the entire energy range. There are no clear-cut methods to unfold the spectrum of resonance states. Therefore we have adopted the procedure that is followed for nuclear resonances and

bound states, namely that the unfolded energy levels $\bar{E}_i$ are calculated from the energy levels in the raw spectrum (E_i) by dividing all the level spacings by the local average spacing [21,22]

$$\bar{E}_{i+1} = \bar{E}_i + (2k+1)\frac{E_{i+1} - E_i}{E_{j_2+1} - E_{j_1}};$$
$$j_1 = i - k, (\overline{i-k} > 0); \quad j_2 = i + k, (\overline{i+k} < n), \tag{1}$$

where k is the number of consecutive spacings used to calculate the local average spacing and n is the total number of energy levels.

From the unfolded spectrum, the nearest neighbor spacing distribution, $P(s)$ can be obtained; the spacings are $\{s_i = \bar{E}_{i+1} - \bar{E}_i, i = 1, 2 \ldots N-1\}$. In the limiting cases of purely chaotic or purely regular systems, the distributions that obtain are well known: the former is (to a high degree of accuracy) given by the Wigner surmise, $P(s) = (\pi s/2)\exp(-(\pi s^2/4))$ [23], while the latter is the Poisson distribution $P(s) = \exp(-s)$ [24].

The spectral rigidity $\Delta_3(L)$, computed from the unfolded spectrum measures the least squares deviation of the staircase function ($N(E)$) from the best straight line in the energy interval of length L [25] and it gives information on the long-range correlations—how one state influences another that is well separated from it. $\Delta_3(L)$ is computed from the unfolded energy values lying in the interval $[0, \ldots, L]$ as [26]

$$\Delta_3(L) = \left\langle \left(\frac{n^2}{16}\right) - \frac{1}{4L}\left(\sum_{i=1}^{n} \bar{E}_i\right)^2 + \frac{3}{8L^2}\left(\sum_{i=1}^{n} \bar{E}_i\right)^2 - \frac{3}{16L^4}\left(\sum_{i=1}^{n} \bar{E}_i^2\right)^2 + \frac{1}{2L}\left(\sum_{i=1}^{n}(n-2i+1)\bar{E}_i\right)\right\rangle, \tag{2}$$

where n is the number of levels within the energy interval L and the ensemble average $\langle\rangle$ is carried out by shifting the box of length L over the entire spectrum. The limiting behaviours are again well-known, and are

$$\Delta_3^{\text{Poisson}}(L) = L/15 \tag{3}$$

and

$$\Delta_3^{\text{GOE}}(L) \approx \frac{1}{\pi^2}\log L - 0.00695 \tag{4}$$

respectively for the regular and chaotic cases [20,23,27–29], the superscript GOE referring to the Gaussian Orthogonal Ensemble of random matrices [20,30]. Molecular systems are often neither purely regular nor purely chaotic, in which case the mixed distribution [31,32] applies,

$$\Delta_3(L; q) = \Delta_3^{\text{Poisson}}((1-q)L) + \Delta_3^{\text{GOE}}(qL), \tag{5}$$

where q represents the fraction of phase space that is chaotic.

For $HeHD^+$ the NNSD distribution, shown in figure 3(a), is more similar to the chaotic case than the regular, indicative of level repulsion. This is confirmed by the behaviour of the $\Delta_3(L)$ statistic, shown in figure 3(b): shown along with the data (triangles) for $HeHD^+$ are the GOE and Poisson values. Except at small L, the computed points for

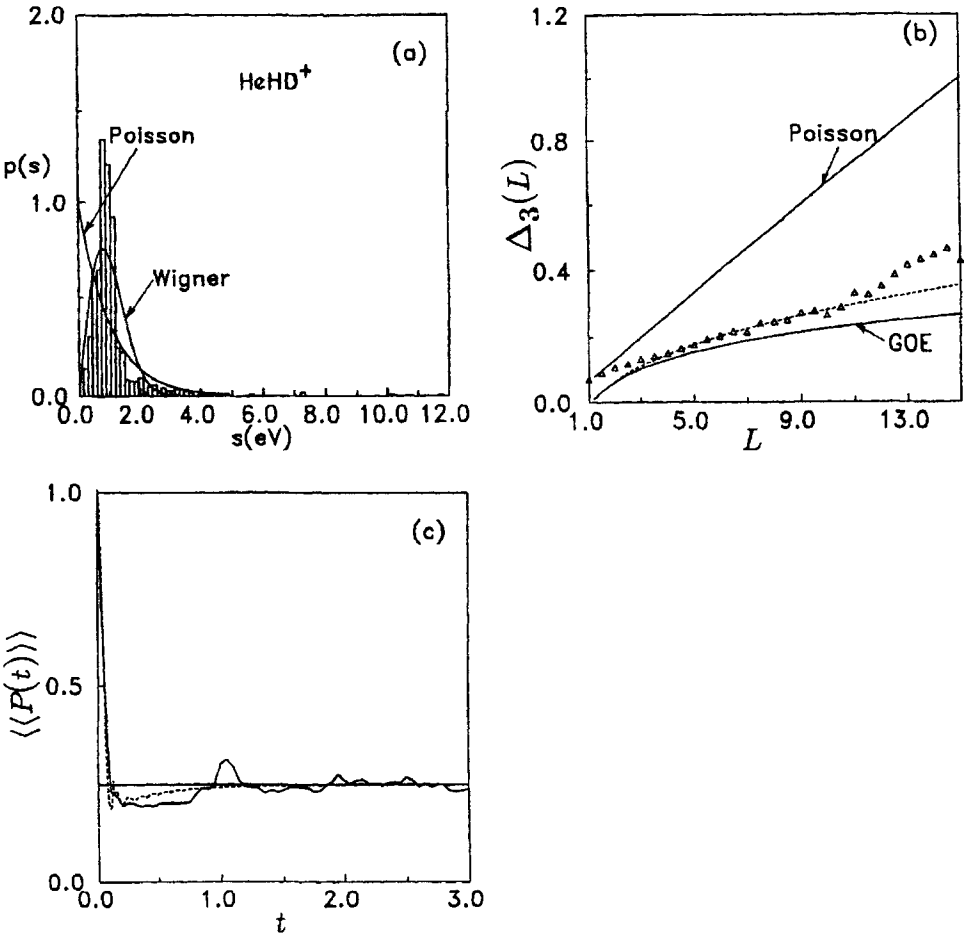

Figure 3. (**a**) The nearest neighbor spacing distribution $P(s)$ derived from the unfolded eigenvalue spectrum for collinear $HeHD^+$, showing short-range correlations. Poisson and Wigner indicate the distributions in the regular and the irregular limits, respectively. (**b**) The spectral rigidity $\Delta_3(L)$ indicating the long-range correlations as a function of the segment length, L, in the above spectrum (triangular points). $\Delta_3(L)$ computed from Eq. 5 for mixed behavior, using $q = 0.9$ is shown by the dashed curve. Poisson and GOE indicate the regular and the irregular limits respectively. (**c**) Variation of ensemble averaged survival probability $\langle\langle P(t)\rangle\rangle$ with time t (in arbitrary units) obtained from the above spectrum (solid curve). The RMT $\langle\langle P(t)\rangle\rangle$ values for $\beta = 0.9$ are included as the dashed curve, for comparison.

$HeHD^+$ are closer to the GOE limit than to the Poisson, thus revealing a high degree of rigidity in the spectrum, more so than the case of collinear (He,H_2^+). Since the computed $\Delta_3(L)$ distribution does not fully correspond to either the Poisson or the GOE value, we have fitted it to the intermediate case (Eq. 5), and obtain the dashed line in figure 3(b), using $q = 0.90$.

For collinear $HeDH^+$ on the other hand, the NNSD in figure 4(a) is more ambiguous: it is difficult to decipher whether it is Poisson-like or Wigner-like. The $\Delta_3(L)$ values

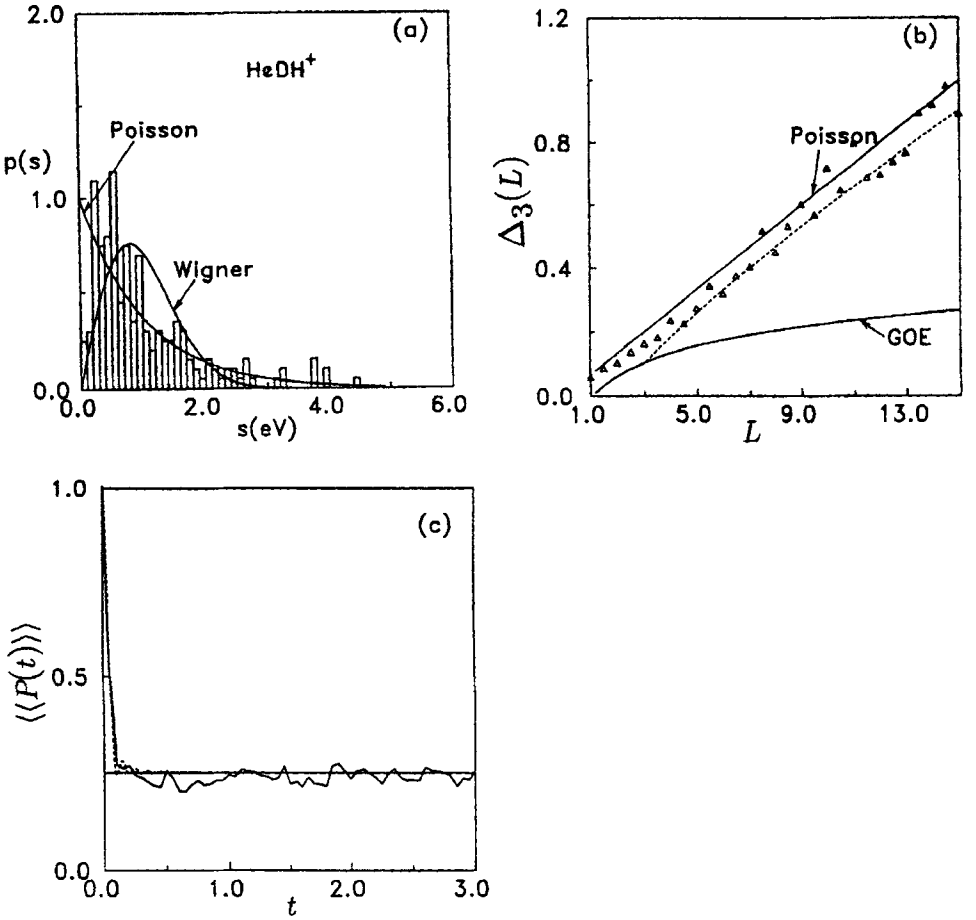

Figure 4. (**a**) The nearest neighbor spacing distribution derived from the unfolded eigenvalue spectrum for collinear $HeDH^+$. (**b**) The spectral rigidity for the same spectrum (triangular points). The dashed curve corresponds to $\Delta_3(L)$ values obtained from Eq. 5 for $q = 0.2$. (**c**) The ensemble averaged survival probability with time t (in arbitrary units), obtained from the above spectrum (solid curve). The RMT$\langle\langle P(t)\rangle\rangle$ values for $\beta = 0.2$ are included for comparison (the dashed curve).

obtained from the unfolded spectrum, shown in figure 4(b) as triangular points, are close to the Poisson distribution. These values are best fitted to Eq. 5 (shown as the dashed curve) using $q = 0.2$, which indicates, in contrast to $HeHD^+$, a high degree of regular behavior.

Further analysis of the dynamical resonance spectra is possible. In the time-domain, analysis of the transition state spectrum proceeds through the computation of the ensemble averaged survival probability $\langle\langle P(t)\rangle\rangle$ [13–16]. The survival probability, averaged over the initial states $\langle P(t)\rangle$, is computed [16] through

$$\langle P(t)\rangle = \frac{3}{N+2}\left\{1 + \frac{2}{3N}\sum_{n,m;n>m}\cos\left[2\pi(\bar{E}_n - \bar{E}_m)\frac{t}{\langle\Delta\bar{E}\rangle}\right]\right\} \tag{6}$$

and further averaging over the Hamiltonian is done by averaging over n levels which are divided into several segments, each containing N levels, to obtain $\langle\langle P(t)\rangle\rangle$. $\langle\Delta\bar{E}\rangle$ is the average level spacing. The $\langle\langle P(t)\rangle\rangle$ values thus obtained from the unfolded spectrum of collinear $HeHD^+$ are shown by the solid curve in figure 3(c). The dip below the asymptotic value at short times ($t \approx 2\pi\hbar/\langle\Delta\bar{E}\rangle$), termed a "correlation hole" is a typical signature of irregularity in the spectrum. The extent of irregularity is estimated by comparing the $\langle\langle P(t)\rangle\rangle$ values with those derived from random matrix theory (RMT) [20]. The latter are obtained from [33]

$$\langle\langle P(t)\rangle\rangle = \frac{3}{N+2}\{1 + \tfrac{1}{3}\triangle_N * [\delta(\tau) - b_{2\beta}(\tau)]\}, \tag{7}$$

where $\tau = t/(2\pi\langle\rho\rangle)\langle\rho\rangle$ is the average level density) and β = 1, 2 and 4 for Gaussian orthogonal, unitary and symplectic ensembles, respectively. $b_{2\beta}(t)$ is the two-level form factor obtained by Fourier transformation of the two-point cluster function, $Y_{2\beta}(\omega)$ [20]. The asterisk implies convolution and $\triangle_N(t) = N^{-1}[\sin(\pi Nt)/\pi t]^2$. If fraction β of the levels obey GOE statistics and (1-β) obey Poisson statistics, $b_{2\beta}$(t) ($0 \leq \beta \leq 1$) is given by [33]

$$b_{2\beta}(t) = \beta b_2(t/\beta) + [(1-\beta)/N]\delta(t) \tag{8}$$

where b_2 indicates the GOE value that is obtained from the two-level cluster function as [20]

$$\begin{aligned} b_2(t) &= 1 - 2|t| + |t|\log(1+2|t|), && |t| \leq 1, \\ &= -1 + |t|\log((2|t|+1)/(2|t|-1)), && |t| \geq 1. \end{aligned} \tag{9}$$

For $HeHD^+$, the $\langle\langle P(t)\rangle\rangle$ values obtained from Eq. 7 for $\beta = 0.9$ (dashed line) are found to be in reasonable agreement with those derived from the spectrum through Eq. 6 (the solid line) as illustrated in figure 3(c). We conclude that approximately 90% of the resonance spectrum for $HeHD^+$ is irregular in nature. This estimate for the fractional irregularity of the eigenvalue spectrum is also in agreement with the estimate obtained from $\Delta_3(L)$ (see above).

For $HeDH^+$ on the other hand, the $\langle\langle P(t)\rangle\rangle$ curve, shown in figure 4(c) reveals only a marginal correlation hole (if any) implying that collinear (He, DH^+) dynamics is highly regular. In addition, the above $\langle\langle P(t)\rangle\rangle$ values, when compared to those obtained from Eq. 7, (the dashed line) yield a value of $\beta = 0.2$, which is consistent with the fractional irregularity of the spectrum obtained from $\Delta_3(L)$.

3. Classical chaos

In order to see how the classical dynamics of the two systems differ we have computed quasiclassical trajectories for both over a wide range of energies. The resulting $P_v^R(E)$ values are included in figures 1 and 2 in the form of dashed lines. As is often the case, the classical threshold (E_{th}^{cl}) values for the exchange reaction in the case of $He + HD^+(v = 0, 1)$ are lower than the quantal (E_{th}^{qm}) values because products with $n_f < 0$ are possible in classical mechanics [34] and are indeed found to be formed. For $v = 2$, $E_{th}^{cl} = E_{th}^{qm}$. For $v = 3$, $E_{th}^{cl} > E_{th}^{qm}$ as the exchange reaction is dynamically

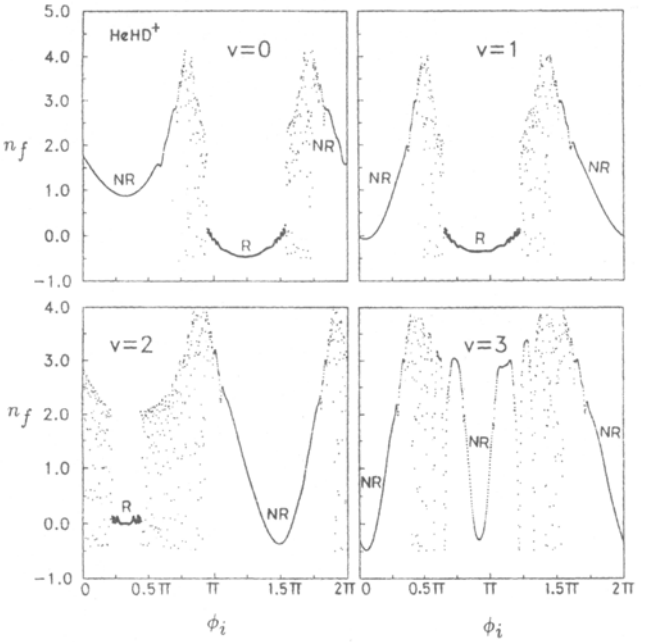

Figure 5. Action-angle plots for a family of 1000 trajectories for various initial vibrational (v) states (indicated in each panel) of HD^+ in collinear $He, HD^+(v)$ collisions at $E_{tot} = 1.0$ eV. R and NR stand for the reactive and the nonreactive band of trajectories, respectively.

forbidden in the vicinity of E_{th}^{qm}. For $He + DH^+(v = 0, 1)$, classical mechanics predicts $P_v^R = 0$ while quantum mechanics yields extremely low (but nonzero) reaction probabilities, P_v^R. For $v = 2$ and 3, $E_{th}^{cl} < E_{th}^{qm}$ as was discussed above. We note, parenthetically, that it is clear that on average, classical mechanics gives a good description of collinear He, HD^+ and He, DH^+ dynamics. The only major discrepancy (over and above the threshold effect) between the classical and quantal results is seen to occur for $He, DH^+(v = 2)$ at high energies and its origin is not clear.

Scattering chaos is most evident [35] when the final quantum number (related to the final classical action) n_f is plotted versus the initial phase, ϕ_i, as shown in figures 5 and 6 for collinear (He, HD^+) and (He, DH^+) collisions for different v states of HD^+ at a total energy (E_{tot}) of 1.0 eV. It is clear from figures 5(a) and 5(b) that there are R and NR bands and chattering regions in between, for $(He, HD^+(v = 0, 1))$. For $v = 2$, the R band has shrunk in size and the chattering region has become wider, when compared to that for $v = 0$ and 1. For $v = 3$, the R band has disappeared completely. There are only NR bands and chattering regions in between. It can be seen that there is a prominent parabola or *icicle* at the centre and there are narrower icicles on either side [36]. A larger number of trajectories computed in the chattering region would reveal fractal characteristics. Since (He, DH^+) collisions are nonreactive for $DH^+(v = 0, 1)$ we obtain only an NR band with slight distortions, as can be seen in figures 6(a) and 6(b). For $v = 2$ and 3 we obtain an NR band and a set of reactive trajectories whose n_f values vary rapidly with ϕ_i. A

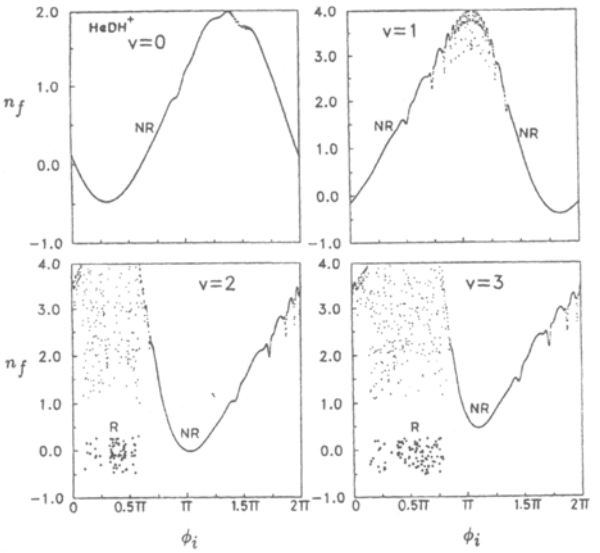

Figure 6. Same as figure 5 for He, $DH^+(v)$ collisions.

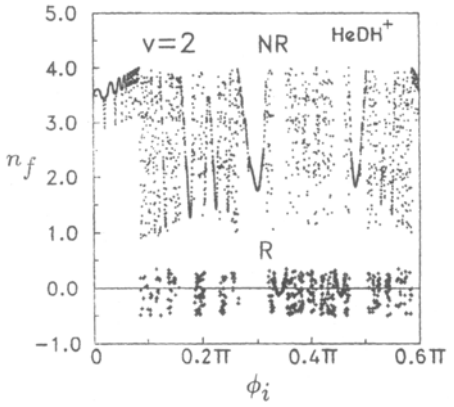

Figure 7. Action-angle plot at increased resolution for He, $DH^+(v = 2)$ collisions. R and NR represent the reactive and the nonreactive trajectories, respectively. The root trajectories that determine the scattering amplitude in the classical S-matrix theory correspond to the intersection of the fractal curve (R) with the line $n_f = 0$; it is evident that there are a very large number (essentially infinite) of these.

blow-up of the chattering region containing reactive trajectories is shown in figure 7. The reactive and the nonreactive trajectories are interspersed along the ϕ_i axis. But because of the differing range of n_f values for the two types of collisions, they are well separated along the vertical axis, but both reactive as well as nonreactive trajectories have characteristic icicle structure. From the point of view of semiclassical S-matrix theory [37], the horizontal line at $n_f = 0$ implies that there is a large number of "root" trajectories and that the expression for the reaction probability would consist of a large

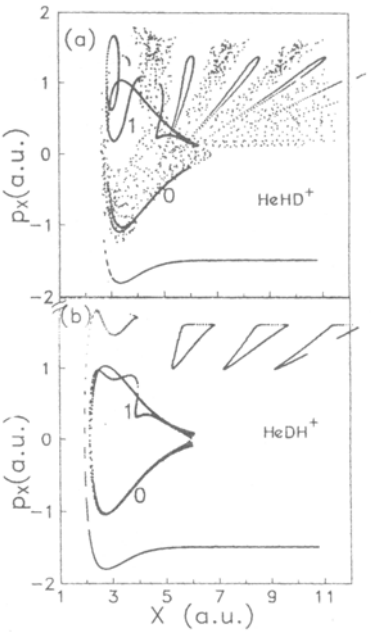

Figure 8. Poincaré surface of section obtained from 400 trajectories superimposed on the zero (0) and the first (1) order separatrices at $E_{tot} = 0.6434$ eV for collinear (**a**) $He, HD^+(v = 0)$ and (**b**) $He, DH^+(v = 0)$ collisions.

number of interference terms, thus explaining the highly oscillatory nature of $P_v^R(E)$ curve for the reaction.

In order to investigate the classical chaos in collinear (He, HD^+) and (He, DH^+) collisions further, we show in figure 8(a) plots of Poincaré SOS for 400 trajectories with $HD^+(v = 0)$ at E_{tot}=0.6434 eV, along with the zero and the first order separatrices. The zero order separatrix is obtained by solving the implicit equation

$$\frac{p_x^2}{2M} + V(x, y = y_e) = 0, \tag{10}$$

where M is the atom-diatom reduced mass and $V(x, y = y_e)$ is the potential energy of the system, with the diatom in its equilibrium configuration. The first order separatrix is obtained by propagating several sets of (x, p_x) values on the zero order separatrix forward in time by setting $y = y_e$ and $p_y = \sqrt{2mE_v}$, where m is the diatomic reduced mass and E_v is the vibrational energy of the diatom, equal to E_{tot}, until it crosses the SOS again. The first order separatrix, when superimposed on the zero order separatrix, reveals a turnstile or broken separatrix [38]. The latter consists of flux-in and flux-out regions. Direct (regular) trajectories never enter the intramolecular bottleneck (identified with the zero order separatrix) whereas indirect (irregular) trajectories do, invariably entering through the flux-in region and exiting through the flux-out region.

The results in figure 8(a) are very similar to those in figure 3 of Ref. [10] for collinear (He, H_2^+) . The regular trajectories never enter the intramolecular bottleneck and they

form a regular elongated baseball bat–like structure in the exit region, owing to a distribution in the final relative translational energy. On the other hand the irregular trajectories enter largely through the broken separatrix and they undergo multiple collisions inside the strong intramolecular bottleneck region and form the complementary dusty pattern between the baseball bats.

The zero and the first order separatrices, along with the Poincaré SOS for a family of regularly sampled 400 trajectories for collinear (He, $DH^+(v=0)$) at E_{tot} =0.6434 eV are shown in figure 8(b). Again, in contrast to figure 8(a), it is clear that all the trajectories are directly scattered. They never enter the intramolecular bottleneck, emphasizing the fact that collinear (He, DH^+) trajectories are predominantly regular at energies below E_{th}^{cl}. Even for energies above E_{th}^{cl}, the Poincaré SOS plots confirm that there are regular and irregular trajectories for collinear He, $HD^+(v=0-3)$. For He, $DH^+(v=0,1)$ the trajectories are nonreactive but entirely regular. For $v=2$ and 3 however, both regular and irregular trajectories occur.

4. Summary and conclusions

Chaotic scattering is sensitive to kinematic effects, and with this in mind, in the present article we have examined the transition state spectra of collinear ($HeHD^+$) and (He, DH^+) systems obtained from time-dependent quantal wave packet calculations. Signatures of quantum chaos become evident in statistical analyses of spacing distributions, the spectral rigidity and ensemble averaged survival probability. In this regard, the two isotopic variants we have looked appear to be dynamically very different, although the interaction potential is identical in both the cases.

The 3-body system (He, H_2^+) has the mass combination Heavy-Light-Light. Changing the terminal atom from H to D, namely by making this a Heavy-Light-Heavy system keeps the dynamics irregular, both classically as well as quantum mechanically. Changing the central atom to D gives the mass combination Heavy-Heavy-Light, and this dramatically reduces the chaotic behaviour: the $HeDH^+$ spectrum is regular despite the wild oscillatory $P_v^R(E)$ curve. Action-angle plots and Poincaré SOS plots indicate that (He, HD^+) dynamics is mixed i.e. partly regular and partly irregular, over the entire energy range of investigation. Results for (He, DH^+), in contrast, suggest that the dynamics is nearly completely regular for $v=0$ and 1, but for $v=2$ and 3, it assumes a mixed character.

As was mentioned in the Introduction, classical chaos and quantum mechanical resonances have been investigated in collinear (H, H_2)[7], (Li, FH) [8] and other systems. Quantal resonances have been reported for three dimensional (He, H_2^+) [2e–2g] and (Li, FH) [39] collisions as well. The large number of spectral lines observed in the infrared predissociation spectrum of H_3^+ [40] have been traced [41] to bound states embedded in the continuum (read transition state resonances) of the H_2–H^+channel and also related to horse-shoe periodic orbits. Indications of the role of kinematic factors in the system came from the D_2H^+ spectra that depended on the formation of H^+/D^+.

Attempts have been made [42] in the past to verify experimentally the existence of resonances in (He, H_2^+) collisions. Following our suggestion [2d] that observables like state-to-state differential cross sections for backward scattering, which are decided

largely by collinear collisions at zero impact parameter, might be amenable to experimental verification, Pollard *et al* [43] measured the same. Unfortunately, their energy resolution (0.15 eV) was not good enough to detect the narrow resonances in the system. Since $P_0^R(E)$ behaves differently for HeH^+ and HeD^+ formation in collinear collisions, it is quite likely that this effect would persist in three dimensions. In that case, measurement of differential cross sections for the two different channels in (He, HD^+) collisions might reveal some of the interesting features reported in this paper.

Acknowledgement

This study was supported in part by a grant from the Commission of European Communities.

References

[1] (a) D G Truhlar (Ed.), *Resonances in electron-molecular scattering, van der Waals complexes and reactive chemical dynamics*, ACS symposium series No. 263, American chemical society, Washington, D. C., 1984
(b) G C Schatz, *Ann. Rev. Phys. Chem.* **39**, 317 (1988)
(c) D E Manolopoulos and D C Clary, *Ann. Rep. Chem. Soc.* **C95**, (1989)
(d) W H Miller, *Ann. Rev. Phys. Chem.* **41**, 245 (1990)
[2] (a) D J Kouri and M Baer, *Chem. Phys. Lett.* **24**, 37 (1974)
(b) J T Adams, *Chem. Phys. Lett.* **33**, 275 (1975)
(c) T Joseph and N Sathyamurthy, *J. Indian Chem. Soc.* **62**, 874 (1985)
(d) N Sathyamurthy, M Baer and T Joseph, *Chem. Phys.* **114**, 73 (1987)
(e) J D Kress, R B Walker and E F Hayes, *J. Chem. Phys.* **93**, 8085 (1990)
(f) J Z H Zhang, D L Yeager and W H Miller, *Chem. Phys. Lett.* **173**, 489 (1990)
(g) B Lepetit and J M Launay, *J. Chem. Phys.* **95**, 5159 (1991)
(h) N Balakrishnan and N Sathyamurthy, *Chem. Phys. Lett.* **201**, 294 (1993); **240**, 119 (1995)
(i) K Sakimoto and K Onda, *Chem. Phys. Lett.* **226**, 227 (1994)
[3] A Kuppermann, J A Kaye and J P Dwyer, *Chem. Phys. Lett.* **74**, 257 (1980)
J Manz, *Comm. At. Mol. Phys.* **17**, 91 (1985)
[4] V Balasubramanian, B K Mishra, A Bahel, S Kumar and N Sathyamurthy, *J. Chem. Phys.* **95**, 4160 (1991)
[5] D R McLaughlin and D L Thompson, *J. Chem. Phys.* **70**, 2748 (1979)
T Joseph and N Sathyamurthy, *J. Chem. Phys.* **86**, 704 (1987)
[6] B B Mandelbrot, *The fractal geometry of nature* (Freeman, New York, 1982)
[7] J R Stine and R A Marcus, *Chem. Phys. Lett.* **29**, 575 (1974)
N Agmon, *J. Chem. Phys.* **76**, 1309 (1982)
[8] A Lagana, M L Hernandez and J M Alvarino, *Chem. Phys. Lett.* **106**, 41 (1984)
[9] H R Mayne and R J Wolf, *Chem. Phys. Lett.* **81**, 508 (1981)
[10] A Rahaman and N Sathyamurthy, *J. Phys. Chem.* **98**, 12481(1994)
[11] S Mahapatra and N Sathyamurthy, *J. Chem. Phys.* **102**, 6057 (1995)
[12] S Mahapatra, R Ramaswamy and N Sathyamurthy, *J. Chem. Phys.* **104**, 3989 (1996)
[13] P Pechukas, *Chem. Phys. Lett.* **86**, 553 (1982)
[14] R D Levine and J L Kinsey, *Proc. Natl. Acad. Sci. (USA)* **88**, 11133 (1991)
[15] J Wilkie and P Brumer, *Phys. Rev. Lett.* **67**, 1185 (1991)
[16] Y Alhassid and R D Levine, *Phys. Rev.* **A46**, 4650 (1992)
[17] V A Mandelshtam, H S Taylor, C Jung, H F Bowen and D J Kouri, *J. Chem. Phys.* **102**, 7988 (1995)
C C Marston, *J. Chem. Phys.* **103**, 8456 (1995)

[18] S Mahapatra and N Sathyamurthy, *J. Chem. Phys.* (submitted)
[19] R S Friedman and D G Truhlar, *Chem. Phys. Lett.* **183**, 539 (1991)
[20] M L Mehta, *Random matrices*, 2nd ed. (Academic, New York, 1990)
[21] S S M Wong and J B French, *Nucl. Phys.* **A198**, 188 (1972)
R Venkatraman, *J. Phys.* **B15**, 4293 (1982)
E Haller, H Köppel and L S Cederbaum, *Chem. Phys. Lett.* **101**, 215 (1983)
D M Leitner, R S Berry and R M Whitnell, *J. Chem. Phys.* **91**, 3470 (1989)
[22] S Mahapatra, *J. Chem. Phys.* **105**, 344 (1996)
[23] *Chaotic behaviour in quantum systems: theory and applications*, edited by G Casati (Plenum press, New York, 1985), Series B: *Physics* Vol. 120
O Bohigas, S Tomsovic and D Ullmo, *Phys. Rep.* **223**, 43 (1993)
Quantum chaos, edited by H Cerdeira, R Ramaswamy, G Casati and M C Gutzwiller (World Scientific Press, Singapore, 1991)
Quantum chaos, edited by G Casati and B V Chirikov, (Cambridge Univ. Press, Cambridge, 1994)
[24] M V Berry and M Tabor, *Proc. R. Soc. London* **A356**, 375 (1977)
[25] F J Dyson and M L Mehta, *J. Math. Phys.* **4**, 701 (1963)
[26] O Bohigas and M-J Gianonni, *Ann. Phys.* **89**, 393 (1975)
[27] T A Brody, J Flores, J B French, P A Mello, A Pandey and S S M Wong, *Rev. Mod. Phys.* **53**, 385 (1981)
Th Zimmermann, L S Cederbaum, H-D Meyer and H Köppel, *J. Phys. Chem.* **91**, 4446 (1987)
[28] O Bohigas, M-J Giannoni and C Schmidt, *Phys. Rev. Lett.* **52**, 1 (1984)
[29] M C Gutzwiller, *Chaos in classical and quantum mechanics* (Springer-Verlag, New York, 1991)
[30] R Ramaswamy, in *Schrödinger centenary surveys in physics*, edited by V Singh and S Lal (World Scientific,Singapore, 1988) pp 236
[31] A Pandey, *Ann. Phys. (NY)* **119**, 170 (1979)
[32] D M Leitner, H Köppel and L S Cederbaum, *J. Chem. Phys.* **104**, 434 (1996)
[33] Y Alhassid and N Whelan, *Phys. Rev. Lett.* **70**, 572 (1993)
[34] S Kumar, N Sathyamurthy and R Ramaswamy, *J. Chem. Phys.* **103**, 6021 (1995)
[35] See, *e.g.* R Ramaswamy, in *Reaction dynamics: recent advances*, edited by N Sathyamurthy (Narosa Press, New Delhi, 1990), pp 101–119
R Ramaswamy, in *Atomic and molecular physics*, edited by A P Pathak (Narosa Press, New Delhi,1992), pp 112–117
[36] K Someda, R Ramaswamy and H Nakamura, *J. Chem. Phys.* **98**, 1156 (1993)
[37] W H Miller, *Adv. Chem. Phys.* **25**, 69 (1974); **30**, 77 (1975)
[38] S R Channon and J L Lebowitz, *Ann. N. Y. Acad. Sci.* **357**, 108 (1980)
R S Mackay, J D Meiss and I C Percival, *Physica* **D13**, 55 (1984)
D Bensimon and L P Kadanoff, *Physica* **DL3**, 82 (1984)
M J Davis and S K Gray, *J. Chem. Phys.* **84**, 5389 (1986)
[39] F Gögtas, G G Balint-Kurti and A R Offer, *J. Chem. Phys.* **104**, 7927 (1996)
[40] A Carrington and R A Kennedy, *J. Chem. Phys.* **81**, 91 (1984)
A Carrington and I R McNab, *Acc. Chem. Res.* **22**, 218 (1989)
[41] M Berblinger, E Pollak and Ch Schlier, *J. Chem. Phys.* **88**, 5643 (1988)
E Pollak and Ch Schlier, *Acc. Chem. Res.* **22**, 223 (1989)
[42] T Turner, O Dutuit and Y T Lee, *J. Chem. Phys.* **81**, 347 (1984)
[43] J E Pollard, J A Syage, L K Johnson and R B Cohen, *J. Chem. Phys.* **94**, 8615 (1991)
J E Pollard, L K Johnson and R B Cohen, *J. Chem. Phys.* **95**, 4894 (1991)